Comparison of $|Q| = 1$ and $|Q| = 2$ Gauge-Field Configurations on the Lattice Four-Torus

Sundance O. Bilson-Thompson,* Derek B. Leinweber,† and Anthony G. Williams‡

CSSM Lattice Collaboration, Special Research Centre for the Subatomic Structure of Matter and The Department of Physics and Mathematical Physics, University of Adelaide, Adelaide SA 5005, Australia

Gerald V. Dunne§

Department of Physics, University of Connecticut, Storrs CT 06269, USA

(Dated: February 1, 2008)

It is known that exactly self-dual gauge-field configurations with topological charge $|Q| = 1$ cannot exist on the untwisted continuum 4-torus. We explore the manifestation of this remarkable fact on the lattice 4-torus for $SU(3)$ using advanced techniques for controlling lattice discretization errors, extending earlier work of De Forcrand *et al* for $SU(2)$. We identify three distinct signals for the instability of $|Q| = 1$ configurations, and show that these signals manifest themselves early in the cooling process, long before the would-be instanton has shrunk to a size comparable to the lattice discretization threshold. These signals do not appear for the individual instantons which make up our $|Q| = 2$ configurations. This indicates that these signals reflect the truly global nature of the instability, rather than the local discretization effects which cause the eventual disappearance of the would-be single instanton. Monte-Carlo generated $SU(3)$ gauge field configurations are cooled to the self-dual limit using an $\mathcal{O}(a^4)$-improved gauge action chosen to have small but positive $\mathcal{O}(a^6)$ errors. This choice prevents lattice discretization errors from destroying instantons provided their size exceeds the dislocation threshold of the cooling algorithm. Lattice discretization errors are evaluated by comparing the $\mathcal{O}(a^4)$-improved gauge-field action with an $\mathcal{O}(a^4)$-improved action constructed from the square of an $\mathcal{O}(a^4)$-improved lattice field-strength tensor, thus having different $\mathcal{O}(a^6)$ discretization errors. The number of action-density peaks, the instanton size and the topological charge of configurations is monitored. We observe a fluctuation in the total topological charge of $|Q| = 1$ configurations, and demonstrate that the onset of this unusual behavior corresponds with the disappearance of multiple-peaks in the action density. At the same time discretization errors are minimal.

PACS numbers: 12.38.Gc, 11.15.Ha, 11.15.Kc

I. INTRODUCTION

Instantons are self-dual classical solutions of the Yang-Mills equations which play several important roles in Quantum Chromodynamics (QCD) [1, 2, 3, 4, 5]. Much is known about their properties and their semiclassical consequences in flat four-dimensional spacetime. On the other hand, at present the most powerful nonperturbative approach to QCD is lattice QCD, where spacetime is discretized. A discrete lattice with periodic boundary conditions is in fact a four-toroidal mesh that approaches a continuum 4-torus in the continuum limit ($a \rightarrow 0$). The properties of instantons on a continuum four-torus $\mathbf{T}^4$ differ in interesting ways from those of instantons on $\mathbf{R}^4$ [6]. In particular, while simple explicit expressions

for multi-instantons are known on $\mathbf{R}^4$ (and on $\mathbf{S}^4$) via the ADHM construction [7, 8], no such concrete results are known on the continuum four-torus. The only known explicit instanton solutions on $\mathbf{T}^4$ are quasi-abelian and of constant field strength [9]. This lack of analytic information gives additional motivation to the study of instantons in lattice QCD, where instanton (*i.e.* self-dual) configurations can be obtained by the technique of cooling, which has the goal of lowering the action S of the configuration without changing its topological charge Q. The action is bounded below by the topological charge (in suitable units), and a numerical instanton configuration is obtained when this bound is saturated.

The *existence* on $\mathbf{T}^4$ of instantons of topological charge $|Q| \geq 2$ was proved long ago by Taubes [10]. However, for periodic boundary conditions it can be proved that $|Q| = 1$ instantons cannot exist on $\mathbf{T}^4$ [11]. This is an elegant corollary of a result known as the Nahm Transform [12], which is an involution that maps an $SU(N)$ instanton of charge Q on $\mathbf{T}^4$ to an $SU(Q)$ instanton of charge N on the dual torus $\hat{\mathbf{T}}^4$. Since $U(1)$ does not support instantons, the Nahm transform implies that $SU(N)$ cannot support $Q = 1$ instantons. The unfortunate lack of exact torus instanton solutions makes explicit study of Nahm's transform difficult, although it has been ver-

*Also at School of Physics, Seoul National University, Seoul 151-747, South Korea; Electronic address: sbilson@physics.adelaide.edu.au
†Electronic address: dleinweb@physics.adelaide.edu.au; URL: http://www.physics.adelaide.edu.au/theory/staff/leinweber/
‡Electronic address: anthony.williams@adelaide.edu.au; URL: http://www.physics.adelaide.edu.au/theory/staff/williams.html
§Electronic address: dunne@phys.uconn.edu

ified in great detail [13] for the quasi-abelian constant field torus instantons. Nahm's construction has been generalized [14] to incorporate twisted boundary conditions, which describe additional non-abelian fluxes [15]. With such twisted boundary conditions it is possible to have a $Q = 1$ instanton solution, and powerful lattice techniques have been developed to numerically implement the Nahm transform including twisted boundary conditions [16]. This is a *tour de force* of lattice gauge theory, as it involves several highly nontrivial numerical steps: cooling the configuration; finding zero modes of an associated Weyl-Dirac operator; reconstructing the Nahm transformed gauge field from the zero modes; and finally probing the self-duality properties of the transformed configuration. The results provide spectacular confirmation of the twisted Nahm transform construction [17, 18].

In this paper we address a somewhat different question, relevant for instantons on an *untwisted* lattice. We accurately cool Monte-Carlo generated configurations in $SU(3)$ with a highly improved action to produce highly self-dual configurations with a range of topological charges. Our goal is to probe in a detailed manner the difference(s) between the behavior under cooling of (un-twisted) configurations with topological charge $|Q| = 1$ and topological charge $|Q| = 2$. The possibility of observing the non-existence of self-dual $|Q| = 1$ configurations in numerical simulations of lattice gauge theory on the 4-torus caught the attention of the lattice QCD community some time ago [19]. There, configurations with $|Q| = 1$ were prepared by cooling Monte-Carlo generated $SU(2)$ configurations with the standard Wilson-Gauge action [20]. The $|Q| = 1$ configurations were then cooled with improved actions toward the self-dual limit and were observed to be unstable to improved cooling. The topological structures were observed to shrink in size and eventually disappear from the lattice. This was proposed as lattice evidence for the non-existence of $|Q| = 1$ instantons on the four-torus [19].

Here, we extend this analysis in several ways, with the goal of identifying and quantifying the impact of the Nahm transform corollary on $|Q| = 1$ configurations in $SU(3)$ gauge theory. We find three distinct signals of instability for the $|Q| = 1$ configurations. Interestingly, these signals appear long before the would-be instantons have shrunk to the point where they "fall through the lattice". Furthermore, we show that these signals occur only for the $|Q| = 1$ configurations, and not for the individual separated lumps that make up our $|Q| = 2$ configurations, which shows that this is really a global rather than a local effect, as expected for the continuum Nahm transform corollary [11].

A key part of our analysis is a precise monitoring and minimizing of lattice discretization errors, which is crucial to interpreting the results of cooling studies. Errors in the discretization of the action can destabilize instantons without regard to the topological charge of the configuration. Improved actions are formulated to algebraically eliminate the leading finite lattice-spacing errors that arise as a result of approximating continuous space-time by a discrete mesh of points. This enables simulations to more accurately approach continuum behavior while still retaining a finite lattice spacing [21]. The use of such improved actions in cooling algorithms has been shown to facilitate high-precision studies of the properties of lattice gauge fields [19, 20, 22, 23].

A convincing demonstration of the instability of $|Q| = 1$ lattice instantons requires careful monitoring of the instanton size *and* discretization errors. These are particularly important, as any instanton with a size smaller than the dislocation threshold of the cooling algorithm is eliminated under improved cooling, again without regard to the topological charge of the configuration. The process is signified by large discretization errors associated with the small size of the object as it falls through the lattice.

This point was recognized as a caveat in the interpretation of the results of Ref. [19], as the size of the topological structures in the configurations studied were initially very close to the dislocation threshold of the cooling algorithm. Thus, it was not possible to determine whether the disappearance of the structure was associated with the Nahm transform corollary, or simply the removal of a dislocation under improved cooling. Our results suggest that this disappearance stage of the topological charge evolution under cooling is in fact the final stage of an instability that manifests itself much earlier in the cooling process, when the topological objects are much larger than the dislocation threshold.

Following from the discussion above, we propose the following criteria to identify convincingly the impact of the Nahm transform corollary:

1. The lattice-discretized cooling action must be accurate with remaining errors acting to stabilize topological structure.

2. The action and topological charge density of a $|Q| = 1$ configuration must be distributed over length scales much larger than the dislocation threshold of the improved cooling algorithm.

3. Evidence must be presented to confirm that discretization errors in the action are minimal where the Nahm transform corollary manifests itself.

4. Evidence that the action of the $|Q| = 1$ configuration is approaching the self-dual limit of $8\pi^2/g^2$ must be provided.

5. Moreover, one must demonstrate that the distribution of action and topological charge distributions are approaching the classical form.

We achieve each of these criteria, in the following manner:

1. We utilize a highly-improved action free from $\mathcal{O}(a^4)$ errors and with slightly positive $\mathcal{O}(a^6)$ errors [22] to ensure the stability of instantons over several thousands of cooling sweeps. This action is known

as a three-loop improved action and appears better adapted to stabilizing topology than the five-loop improved action.

2. The size of the action and topological charge distributions are estimated by fitting the shape of the distribution surrounding the peak of the distribution to the classical single-instanton density profile. The position and size, ρ, of the distributions are determined and compared with the dislocation threshold of the cooling action.

3. Remaining lattice discretization errors are evaluated by comparing the $\mathcal{O}(a^4)$-improved gauge-field action with an $\mathcal{O}(a^4)$-improved "reconstructed action" obtained from the square of an $\mathcal{O}(a^4)$-improved lattice field-strength tensor [22], thus having different $\mathcal{O}(a^6)$ discretization errors.

4. Action and "reconstructed action" results will be reported in units of the single instanton action $S_0 = 8\pi^2/g^2$.

5. During the cooling process we also monitor the number of peaks in the action density. Even as the action approaches the single instanton action, numerous peaks in the action density can be identified. Their position and size are also monitored as a function of cooling sweep.

This paper is set out as follows. In Section II we briefly describe the highly-improved lattice discretization of the continuum action, field-strength tensor, reconstructed action, and topological charge operators. In Section III we outline the simulation techniques and parameters. Section IV examines the evolution of $|Q| = 1$ configurations under improved cooling and puts the results in perspective through a direct comparison with the behavior of $|Q| = 2$ configurations. Our conclusions are presented in Section V.

II.   LATTICE ACTION AND TOPOLOGICAL CHARGE OPERATORS

The lattice version of the Yang-Mills action was first proposed by Wilson [24]. The action is calculated from the plaquette, $W_{\mu\nu}^{(1\times 1)}$, a closed product of four link operators incorporating the link U_μ,

$$S_{\text{Wil}} = \beta \sum_x \sum_{\mu<\nu} \left(1 - \frac{1}{N} Re\,\text{tr}\, W_{\mu\nu}^{(1\times 1)}(x)\right), \quad (1)$$

$$= \frac{1}{2} \int d^4x\,\text{tr}\, F_{\mu\nu}^2(x) + \mathcal{O}(a^2), \quad (2)$$

provided $\beta = 2N/g^2$ for an $SU(N)$ field theory. We will use the notation $W_{\mu\nu}^{(m\times n)}$ to denote the closed loop product (Wilson loop) in the $\mu-\nu$ plane with extent m lattice spacings in the μ-direction and n lattice spacings in the

ν-direction. Similarly, the lattice topological charge is obtained by summing the charge density over each lattice site,

$$Q = \sum_x \frac{g^2}{32\pi^2} \epsilon_{\mu\nu\rho\sigma}\,\text{tr}\{F_{\mu\nu}(x)F_{\rho\sigma}(x)\} \quad (3)$$

where μ, ν, ρ, σ sum over the directions of the lattice axes.

Since the action and topological charge constructed from different Wilson loops have different $\mathcal{O}(a^2)$ and higher terms we may cancel leading discretization errors by combining the contributions of different loops. For example, de Forcrand et al. [19, 20] have used tree-level improvement to construct a lattice action which eliminates $\mathcal{O}(a^2)$ and $\mathcal{O}(a^4)$ errors, by using combinations of up to five Wilson loop operators, which we denote $L_1, ..., L_5$. In the case of rectangular loops $m \neq n$ the contribution of the loops in each direction is averaged, so that

$$
\begin{aligned}
L_1 &\equiv W_{\mu\nu}^{(1\times 1)}, \\
L_2 &\equiv W_{\mu\nu}^{(2\times 2)}, \\
L_3 &\equiv \frac{1}{2}\left\{W_{\mu\nu}^{(2\times 1)} + W_{\mu\nu}^{(1\times 2)}\right\}, \\
L_4 &\equiv \frac{1}{2}\left\{W_{\mu\nu}^{(3\times 1)} + W_{\mu\nu}^{(1\times 3)}\right\}, \\
L_5 &\equiv W_{\mu\nu}^{(3\times 3)}.
\end{aligned}
\quad (4)
$$

The improved action of de Forcrand et al. is a linear combination of the Wilson actions calculated from $L_1, ..., L_5$, each divided by the relevant loop area squared (in units of a^4), and respectively weighted by the constants

$$
\begin{aligned}
c_1 &= (19 - 55c_5)/9, \\
c_2 &= (1 - 64c_5)/9, \\
c_3 &= (640c_5 - 64)/45, \\
c_4 &= 1/5 - 2c_5,
\end{aligned}
\quad (5)
$$

with c_5 as a free variable, i.e.,

$$S = c_1 S(L_1) + \frac{c_2}{16}S(L_2) + \frac{c_3}{4}S(L_3) + \frac{c_4}{9}S(L_4) + \frac{c_5}{81}S(L_5). \quad (6)$$

Selecting appropriate values for c_5 enables one to set the contribution of certain loops to zero, creating so-called 3-loop ($c_5 = 1/10$), or 4-loop ($c_5 = 0$) improved actions. Other values of c_5 lead to 5-loop improved actions. Following Ref. [19, 20], we consider $c_5 = 1/20$ (midway between the 3-loop and 4-loop values) to define the "standard" 5-loop action.

All of these actions have the same level of improvement, but in general they will have different $\mathcal{O}(a^6)$ errors. We refer to the Wilson action, Eq. (2), constructed from the plaquette as a 1-loop action. A 2-loop action may be constructed [25] from $\frac{5}{3}L_1 - \frac{1}{6}L_3$. These definitions of the variously-improved actions are used in our cooling algorithm.

We construct a highly-improved lattice field-strength tensor, analogously to the construction of the cooling ac-

tion. The relations

$$W_{\mu\nu}^{(1\times1)} = \left\{1 + ig\oint A.dx - \frac{g^2}{2}(\oint A.dx)^2 + \mathcal{O}(g^3)\right\},$$

$$W_{\mu\nu}^{(1\times1)\dagger} = \left\{1 - ig\oint A.dx - \frac{g^2}{2}(\oint A.dx)^2 + \mathcal{O}(g^3)\right\},$$

indicate the field-strength tensor may be accessed via

$$\frac{-i}{2}\left(W_{\mu\nu}^{(1\times1)} - W^{(1\times1)\dagger} - \frac{1}{3}\mathrm{tr}\left(W_{\mu\nu}^{(1\times1)} - W_{\mu\nu}^{(1\times1)\dagger}\right)\right)$$
$$= g\oint A.dx + \mathcal{O}(g^3)$$
$$= ga^2 F_{\mu\nu}(x_0) + \mathcal{O}(ga^4) + \mathcal{O}(g^3 a^4), \qquad (7)$$

where we have subtracted one-third of the trace to enforce the traceless aspect of the Gell-Mann matrices. As with the improved action, the improved field-strength tensor is constructed from a combination of Wilson loops. Our improved field-strength tensor is given by

$$g\,F_{\mu\nu}^{\mathrm{Imp}} = \left[k_1 C_{\mu\nu}^{(1,1)} + k_2 C_{\mu\nu}^{(2,2)} + k_3 C_{\mu\nu}^{(1,2)} + \right.$$
$$\left. k_4 C_{\mu\nu}^{(1,3)} + k_5 C_{\mu\nu}^{(3,3)}\right], \qquad (8)$$

where $C_{\mu\nu}^{(m,n)}$ are the clover averages of $m \times n$ and $n \times m$ path-ordered link products [22]. The improvement constants take the values

$$k_1 = 19/9 - 55k_5,$$
$$k_2 = 1/36 - 16k_5,$$
$$k_3 = 64k_5 - 32/45,$$
$$k_4 = 1/15 - 6k_5,$$

and in this case k_5 is the tunable free parameter. $F_{\mu\nu}^{\mathrm{Imp}}$ may be inserted directly into Eq. (3) to create an improved topological charge operator, or into the equation [22, 26]

$$S_R = \beta \sum_x \sum_{\mu,\nu} \frac{1}{12}\,\mathrm{tr}\,\left[g^2\,F_{\mu\nu}^2(x)\right]. \qquad (9)$$

to create a "reconstructed" improved action, S_R. Both improved operators will have errors of $\mathcal{O}(a^6)$. Errors associated with g are rapidly suppressed in the process of cooling. Appropriate choices of k_5 enable us to create 3-loop or 4-loop improved versions of the field-strength. Our 5-loop improved field-strength tensor is defined with $k_5 = 1/180$, midway between the 3-loop and 4-loop values of $k_5 = 1/90$ and 0 respectively [22]. While the 5-loop improved field-strength tensor is marginally more accurate, it is computationally expensive. We adopt the 3-loop improved field-strength tensor to construct the $\mathcal{O}(a^4)$-improved topological charge and reconstructed action operators.

Tadpole corrections to the improvement coefficients [25] are included and updated after every cooling sweep.

Our experience [22] is that tadpole improvement factors are beneficial in the early stages of cooling and remain beneficial even as $u_0 \to 1$.

Previous investigations [22] have indicated the 3-loop and 5-loop improved actions are similarly accurate in reproducing the classical action of approximately self-dual configurations. In some cases, the 5-loop action would underestimate the classical action. Such errors open the possibility of destabilizing topological structures over several thousand cooling sweeps, regardless of the topological charge of the configuration. For the configurations investigated in Ref. [22] the errors in the 3-loop improved action were consistently positive; thus acting to stabilize topology. In the following, we adopt the 3-loop improved action.

III. LATTICE APPROACH

To investigate the stability of self-dual gauge field configurations on the (untwisted) 4-torus, we construct an ensemble of field configurations using the Cabibbo-Marinari [27] pseudo-heatbath algorithm with three diagonal $SU(2)$ subgroups looped over twice. We thermalize for 5000 sweeps with an $\mathcal{O}(a^2)$-improved action from a cold start (all links set to the identity) and select configurations every 500 sweeps thereafter [28]. Configurations are numbered consecutively in the order that they are produced in the Markov-chain process. Hence configuration 1 was saved after 5000 thermalization sweeps from a cold start, configuration 2 was saved 500 sweeps after configuration 1, and so on. Our results are generated on a $12^3 \times 24$ periodic lattice at $\beta = 4.60$, with a lattice spacing of $a = 0.122(2)$ fm determined by a string tension analysis incorporating the lattice coulomb term. Cooling is performed with a 3-loop improved action with tadpole improvement (using the plaquette definition of the mean link) and the topological charge is assessed with the 3-loop improved operator. Links which may be updated in parallel are identified and partitioned [29]. Updating the partitioned links in parallel minimizes the drift of objects in the cooled configurations.

As a thermalized configuration is cooled, over the course of many hundreds of sweeps the action S of the configuration monotonically decreases. This occurs because the cooling algorithm smooths out short-range fluctuations in the field. As the high-frequency components of the field are suppressed the underlying semi-classical structure of the field is revealed. If cooling proceeds for long enough the configurations will become self-dual consisting only of instantons or anti-instantons.

The action, S, is bounded below by the magnitude of the topological charge, Q, i.e.,

$$S \geq S_0\,|Q| = \frac{8\pi^2}{g^2}\,|Q|, \qquad (10)$$

where in the continuum Q assumes an integer value [3, 4].

The quantity $S_0 = \frac{8\pi^2}{g^2}$ is the action associated with a single instanton and is independent of the instanton size.

As cooling is applied uniformly over the 4-volume of the torus, configurations become locally self-dual. In the infinite volume limit where well-separated instantons and anti-instantons can simultaneously be present, the total action and topological charge will approach discrete values, satisfying the relations $S/S_0 = n_I + n_A$ and $Q = n_I - n_A$, where n_I and n_A are the number of instantons and anti-instantons present respectively. On a finite volume, one might expect to see some plateauing in the action density as a function of cooling sweep, when these conditions are satisfied. However, further cooling will lead to the annihilation of instanton–anti-instanton pairs in the finite volume, until only instantons or only anti-instantons remain. The configuration will then continue to cool until it achieves complete global self-duality, i.e., $S/S_0 = |Q|$.

As discussed in the Introduction, self-dual configurations with $|Q| = 1$ (*i.e.* a single instanton or a single anti-instanton) do not exist on the untwisted continuum four-torus [11]. Note, of course, that configurations with topological charge $|Q| = 1$ do exist; they just cannot be made self-dual. In other words, the lower bound $S \geq S_0$ cannot be exactly saturated. We therefore expect to see different behavior of $|Q| = 1$ and $|Q| = 2$ lattice configurations under cooling. The next section is devoted to a study of signatures of this different behavior.

IV. COOLING COMPARISON FOR $Q = 1$ AND $Q = 2$ CONFIGURATIONS

A. Action and Charge Evolution

Throughout the discussion of the results we will use the following notation: the cooling action will be denoted by S, the reconstructed action by S_R and the topological charge by Q. The type of improvement scheme used will be denoted by a number in parentheses. Hence the 2-loop improved cooling action, constructed from L_1 and L_3 is written as $S(2)$, our topological charge calculated from a 3-loop improved field-strength tensor is written as $Q(3)$, our 3-loop reconstructed action (calculated from a 3-loop improved field-strength tensor) is written as $S_R(3)$, and so on. The action reported throughout the cooling process will typically be divided by S_0 to facilitate the comparison with $|Q|$. Hence the curves in figures labeled as $S(n)$ and $S_R(n)$ actually represent the normalized action values $S(n)/S_0$ and $S_R(n)/S_0$ respectively.

1. $|Q| = 1$ Configurations

In Fig. 1 we show $S(3)/S_0$ and $|Q(3)|$ for configuration 64. After a small number of cooling sweeps this configuration rapidly settles down to a topological charge of one. Hence we expect that under continued cooling with
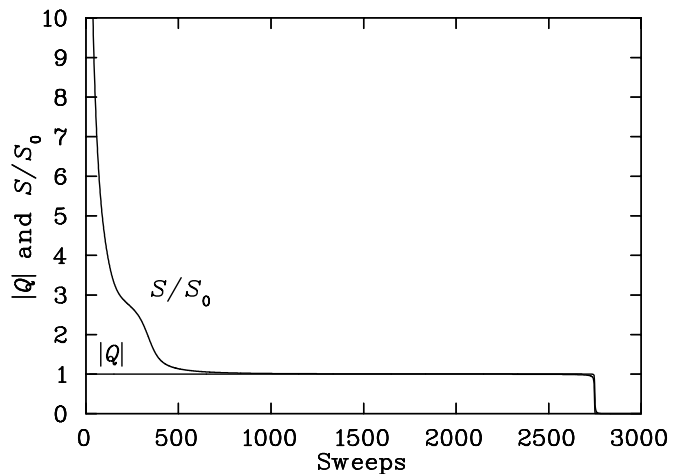

FIG. 1: Topological charge, $Q(3)$, and normalized action, $S(3)/S_0$, for configuration 64. Notation is described in the text. In particular, Q and S are assessed here with the 3-loop improved topological charge and action operators. The action evolution flattens around 300 sweeps characteristic of a well separated instanton anti-instanton pair. Annihilation of the instanton anti-instanton pair follows as signified by the reduction of the action by two units, while the topological charge remains unchanged. The nearly self-dual single instanton configuration destabilizes around sweep 2700.

negligible discretization errors, it should never reach true self-duality. We do observe a long plateau where the configuration appears to closely approach self-duality. However, around cooling sweep 2700 it eventually destabilizes and collapses to triviality. This behavior is consistent with earlier results [19] for $SU(2)$. We will argue in the following that this final destabilization of the instanton is in fact the final stage of a series of evolution stages, with this final disappearance of the would-be instanton being due to its small size relative to the dislocation threshold of the cooling algorithm.

Let us now examine the same configuration with an enhanced vertical scale as in Fig. 2. The configuration fails to achieve self-duality before it destabilizes and becomes trivial. However, a very high level of accuracy is obtained for the topological charge, Q, between sweeps 200–400. This is the region in which the action evolution flattens with $S/S_0 \simeq 3$ signaling approximate local self-duality. This region provides a benchmark for the level of accuracy that may be achieved through the use of highly improved operators.

For sweeps 400-1400 we see the value of Q rise away from the integer value of one. This "cresting behavior" commences at the same time that the action leaves the regime of $S/S_0 \simeq 3$ and approaches the classical instanton action. We note that it is well separated from the ultimate collapse of the configuration.

The two 3-loop improved actions ($S(3)$ and $S_R(3)$) remain greater than $S_0|Q|$ as required. The two actions deviate significantly from one another when the configu-

ration collapses to triviality, which is indicative of large discretization errors. Thus, this destabilization, at this stage of the cooling process, should not be attributed to the Nahm transform corollary. In contrast, the two action measures agree relatively well even at the peak in the topological charge cresting. Note that $S(3)/S_0 > 1$, so that errors should act to stabilize the configuration.

To illustrate the reproducible nature of these results we also present results in Fig. 3 for configuration 11; another $|Q| = 1$ configuration. Beyond 200 sweeps, the behavior is nearly identical. Beyond approximately 1500 cooling sweeps we see a crossing followed by a large divergence of the action values and a sudden drop in the topological charge. This indicates the onset of severe discretization errors, again suggesting a small size for the nontrivial topological structure, the "would-be" instanton.

Based on these results, we propose that the cresting of the topological charge early in the cooling process, and associated with the departure of $S(3)/S_0$ from the regime of 3 toward 1, is a distinct signature of the ultimate instability of the single instanton on the lattice. The eventual disappearance of the would-be instanton happens much later in the cooling process, and appears to rather be a consequence of large discretization errors in that region. In the next sub-section, we contrast this directly with the behavior of $|Q| = 2$ configurations under cooling.

2. $|Q| = 2$ Configurations

To show that this cresting behavior is specific to $|Q| = 1$ configurations, we compare one and two instanton configurations in Figs. 4 and 5. In these figures we consider the three-loop quantities $S(3)/S_0$ and $|Q(3)|$. For the two-instanton case, we plot $(S(3)/S_0) - 1$ and $|Q(3)| - 1$, so that the curves for the $|Q| = 1$ and $|Q| = 2$ cases may be directly compared. The level of self-duality achieved by the two-instanton configurations is far superior to that of the single-instanton configurations. The cresting behavior observed in the topological charge of the $|Q| = 1$ configurations is not seen at all for the $|Q| = 2$ configurations.

We stress that the behavior of the $|Q| = 1$ configurations differ significantly from that of the $|Q| = 2$ configurations long before the $|Q| = 1$ configurations collapse to triviality. Indeed, this deviation becomes manifest relatively early in the cooling process. For configuration 64 of Figs. 1 and 2 the cresting behavior begins as the number of locally self-dual objects on the lattice drops from three to one.

To confirm the consistency of this picture, it is important to know the size of these objects in order to evaluate whether the dislocation threshold of the cooling algorithm is playing a role in the evolution of the configurations, and at what stage of the cooling process this is important. This is the subject of the next section.
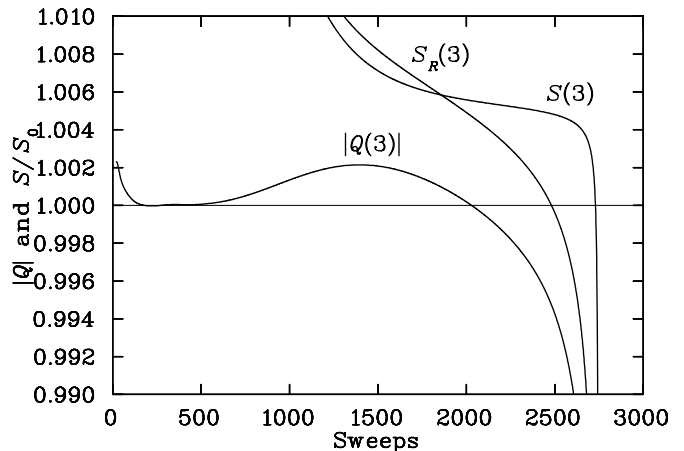

FIG. 2: Plot showing the fine detail of the $|Q| = 1$ configuration illustrated in Fig. 1; configuration 64. The three-loop cooling action, $S(3)$, three-loop reconstructed action, $S_R(3)$, and the three-loop topological charge, $Q(3)$ are plotted. A very high level of accuracy is obtained for the topological charge between sweeps 200–400. A "cresting behavior" appears as S/S_0 drops from ~ 3 toward 1.
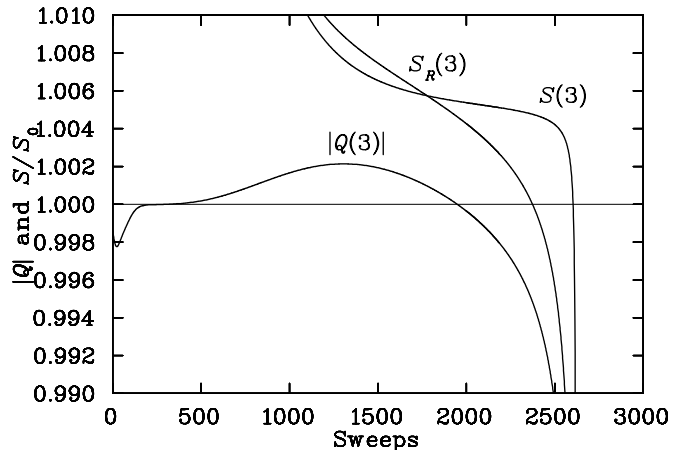

FIG. 3: The fine detail of another $|Q| = 1$ configuration; configuration 11. Beyond 200 sweeps, the behavior is nearly identical to that illustrated in Fig. 2.

B. Instanton size evolution

To investigate further the behavior of the topological structure of these $|Q| = 1$ and $|Q| = 2$ configurations under cooling, we implement an algorithm which identifies local peaks in the action and topological charge densities. Peaks in the action density are identified by finding a point at the center of a 3^4 hypercube whose action density exceeds that of the neighboring 80 points of the hypercube. The algorithm may also be applied to the topological charge density in two steps, reversing the sign of the topological charge density to convert valleys
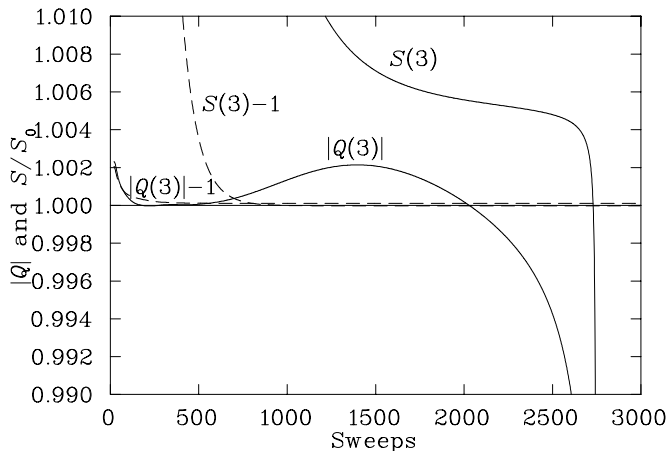
FIG. 4: Comparison of the $|Q| = 1$ configuration (configuration 64, solid line) with a $|Q| = 2$ configuration (configuration 90, dashed line). For the two-instanton configuration both $S(3)/S_0$ and $|Q|$ have been reduced by unity so that the curves may be directly compared with the $|Q| = 1$ configuration. The accurate behavior of the two-instanton configuration contrasts the single-instanton case.
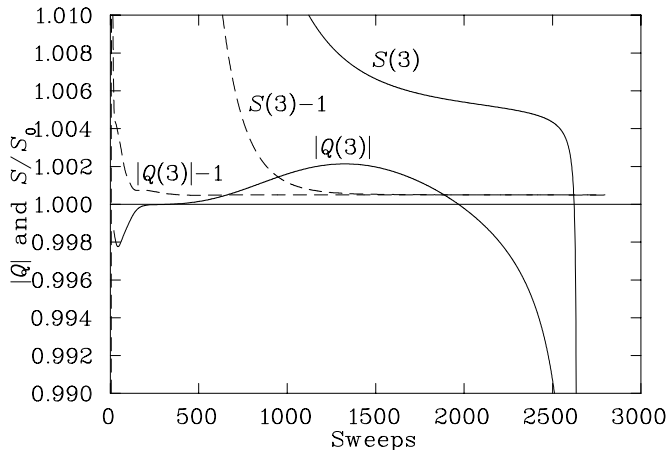

FIG. 5: A similar comparison of a $|Q| = 1$ configuration (configuration 11, solid line) with a $|Q| = 2$ configuration (configuration 27, dashed line). As in Fig. 4, $S(3)/S_0$ and $|Q|$ for the two-instanton configuration have been reduced by unity to allow a direct comparison of the curves with the $|Q| = 1$ configuration.

to peaks.

The algorithm then fits the structure of the gauge fields around these peaks to the classical instanton form for the action density

$$S(x) = \xi \, \frac{6}{\pi^2} \, \frac{\rho^4}{((x - x_0)^2 + \rho^2))^4} \,, \qquad (11)$$

generalized by the inclusion of ξ to allow for an overall normalization different from 1 due to periodic images

of the action density [30]. For an instanton in infinite volume on $\mathbf{R}^4$, $\xi = 1$. The fit parameters returned by this algorithm are the coordinates of the center of each instanton-like peak, x_0, the instanton-size parameter for each peak, ρ, and the overall scale factor for the peak, ξ.

It should be noted that not every peak found by this algorithm is an instanton, particularly during the early stages of the cooling process. However, we certainly anticipate that the peaks which survive under cooling will approach the form of instantons or anti-instantons as the cooling proceeds. Peaks which do not correspond to instanton-like structures will disappear in the early stages of cooling. Of the larger would-be instantons and anti-instantons surviving these early cooling steps, all but $|Q|$ of them will ultimately disappear due to the annihilation of instanton–anti-instanton pairs.

We use this algorithm to investigate the topological properties of configurations 11 and 64 (corresponding to $|Q| = 1$) and in configurations 27 and 90 (corresponding to $|Q| = 2$). In Fig. 6 we illustrate how the instanton size, ρ, varies with sweep number for configurations 64 and 11. Three initial instanton-like peaks are identified in configuration 64 and four are identified in configuration 11. The solid line in each of these figures denotes the peak which survives long-term cooling and becomes the approximately self-dual object in each configuration. The dashed lines denote the temporary peaks, which disappear under cooling.

In configuration 64 we see that all peaks rapidly grow in size initially. Both of the temporary peaks are seen to expand in size with the associated peak height decreasing until the peaks "melt" away. These peaks are associated with the plateau in the action observed in Fig. 1. Hence we see that topological objects can disappear on the lattice by "melting away" where $\rho \to \infty$, which is a different mechanism from the behavior of "falling through the lattice" where $\rho \to 0$.

The remaining topological object reacts by slowing its growth. Once all of the other structures have disappeared, the surviving object shrinks rapidly. In minimizing its size relative to the finite volume of the 4-torus, the object can best approximate the self-dual nature of an instanton and temporarily evade the ultimate consequence of the Nahm transform. The rate of shrinkage is related to the size of the object. The shrinkage slowly continues until the instanton size is approximately two lattice spacings, at which time the object is smaller than the dislocation threshold of the cooling algorithm and is rapidly suppressed.

Similar results are observed for configuration 11 (another $|Q| = 1$ configuration), as shown in the lower plot of Fig. 6. Again all peaks rapidly grow in size initially, but as each of the three temporary peaks expands and "melts away", the single instanton reacts by slowing its growth. Once all of the other structures have disappeared, we see that the surviving single (anti-)instanton shrinks rapidly due to its large size. The shrinkage continues until the dislocation threshold is encountered, at which point it is
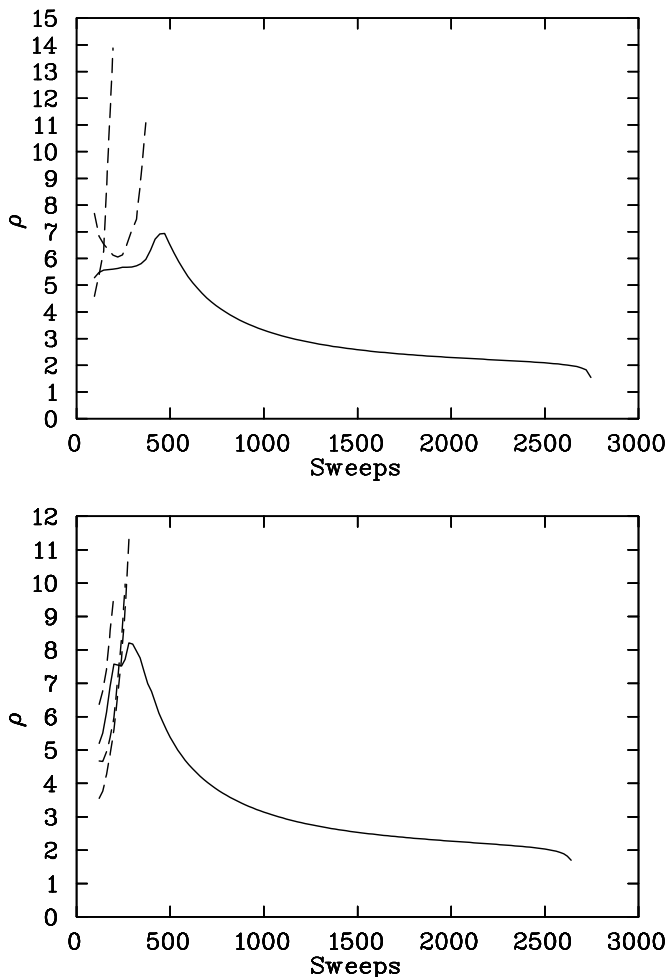
FIG. 6: Size of the single instanton (ρ measured in lattice units) in configuration 64 (upper figure) and configuration 11 (lower figure). An abrupt change in the size evolution occurs as other peaks in the distribution disappear through the process of "melting" as described in the text. After sweep 2500 the instanton in each configuration rapidly disappears and hence the associated size parameter cannot be measured accurately. Dashed lines represent the size of transitory peaks.

rapidly suppressed.

The point of inflection seen in the evolution of the single-instanton size around 1900 sweeps in Fig. 6 signifies the dislocation threshold of the S(3) improved cooling algorithm. For both configurations $\rho \simeq 2.2$ at the point of inflection. This dislocation threshold is similar to $\rho_{\mathrm{D}} = 2.23$ for $S(5)$ as determined in Ref. [19].

In the continuum infinite volume limit, instantons have no implicit scale and can be any size with the same action S_0. On a finite 4-torus in the continuum, the only relevant quantity is the relative size of the instanton to the 4-torus size. On the continuum 4-torus, we therefore expect that in the limit where the size of the would-be instanton vanishes with respect to the 4-torus size, it should able to approach arbitrarily closely to self-duality. Thus,

under continued cooling on the lattice a $|Q| = 1$ configuration will approach the self-dual limit by decreasing its size. As it does so, discretization errors will become increasingly large until the object encounters the dislocation threshold, at which point the object will be removed by the cooling algorithm. This is the ultimate fate of a $|Q| = 1$ configuration under cooling.

In both $|Q| = 1$ cases, the onset of the cresting in the topological charge occurs when the size of the object is seven to eight lattice spacings, well above the size of two lattice spacings where the dislocation threshold of the cooling algorithm removes the objects. Thus, at the onset of the cresting of $|Q|$ the objects are large enough that the dislocation threshold of the cooling algorithm is irrelevant. Since the cresting behavior appears to be a distinct signal of the ultimate disappearance of the $|Q| = 1$ objects, this suggests that the dislocation threshold is not the primary reason for the instability of the $|Q| = 1$ configurations, even though it is the reason for its final disappearance.

To make this even more concrete, we contrast these results for the size dependence of the $|Q| = 1$ objects under cooling, with the corresponding results for the $|Q| = 2$ configurations.

The sizes of the two instantons in each of configurations 27 and 90 (which each have $|Q| = 2$) are shown in Fig. 7. First, note that in each case the configuration consists of two identifiably separate topological objects, rather than one single object of instanton number 2. For each configuration, the two instantons drift apart under cooling, appearing to repel one another. More interestingly, in each case, the size of one instanton grows while the other shrinks, until they each settle (after roughly 1000 sweeps) to approximately the same size. We do not know if this behavior is necessary – however, the fact that the same thing happened in these two independent cases is suggestive. Perhaps this symmetry between the sizes of the cooled two-instanton configuration is due to an image effect that balances two objects at equal sizes roughly at "opposite ends" of the lattice. It would be interesting to probe this question more deeply, both on the lattice and for the continuum four-torus. For example, for $SU(2)$ ADHM instantons on $\mathbf{R}^4$ it is known that the behavior of $Q = 2$ instantons depends crucially on the relative $SU(2)$ orientation of the two constituent instantons, which has important implications for the instanton size distribution [31].

Another striking contrast between the size-dependence of the $|Q| = 2$ and $|Q| = 1$ configurations is that the $|Q| \simeq 1$ objects shrink in size by a factor of approximately three as the cooling proceeds over the course of two thousand sweeps, while in the $|Q| = 2$ configurations, each object changes size by no more than 10%. This indicates a significant level of stability throughout most of the course of the cooling process. Since the $|Q| = 2$ configurations consist of two distinct topological objects, each of which may be thought of as a single instanton, it is striking that for these configurations the single in-
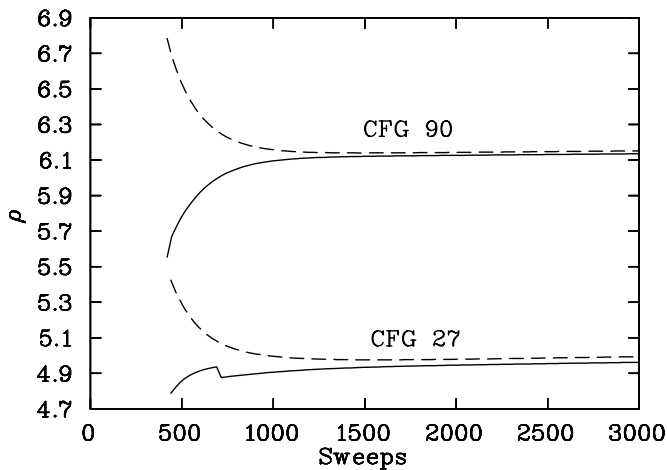
FIG. 7: Size evolution of the two instantons (ρ measured in lattice units) in configuration 27, and the two instantons in configuration 90. The solid and dashed lines represent the size of one of the two instantons present in each configuration. The discontinuity in the lower figure (configuration 27) is believed to be caused by a sudden change in parameter values as the fitting program used to calculate the single instanton size from our lattice data jumped from one local χ^2 minimum to another.

stantons do not shrink in the same way that the $|Q| = 1$ would-be instantons do. This shows that the distinction between the $|Q| = 1$ and $|Q| = 2$ configurations is really a global effect, not a local one, and this is exactly what we would expect from the Nahm transform corollary [11]. So, this difference in the size dependence under cooling is another signal (in addition to the cresting behavior of $|Q|$ identified in the previous section) of the instability of $|Q| = 1$ configurations under cooling, and once again we note that the difference can be seen already very early in the cooling process, rather than just at the late time when the $|Q| = 1$ objects vanish due to discretization errors.

C. Discretization Errors

In this last section we identify a third distinct signal of the instability of the $|Q| = 1$ configurations under cooling, and show that it can also be seen early in the cooling process. It was noted already in Figs. 2 and 3 that S and S_R diverge rapidly in the period prior to the collapse of the $|Q| = 1$ configurations. Actually, for the $|Q| = 1$ configurations, the deviation between these two actions appears much earlier, as is shown in Fig. 8. In Fig. 8 we present plots of the ratio of S to S_R, for both $|Q| = 1$ configurations (11 and 64) and $|Q| = 2$ configurations (27 and 90). Since the cooling action and reconstructed action are improved differently, they are expected to have different $\mathcal{O}(a^6)$ discretization errors. The ratio of S to S_R therefore indicates the relative scale of the $\mathcal{O}(a^6)$ errors
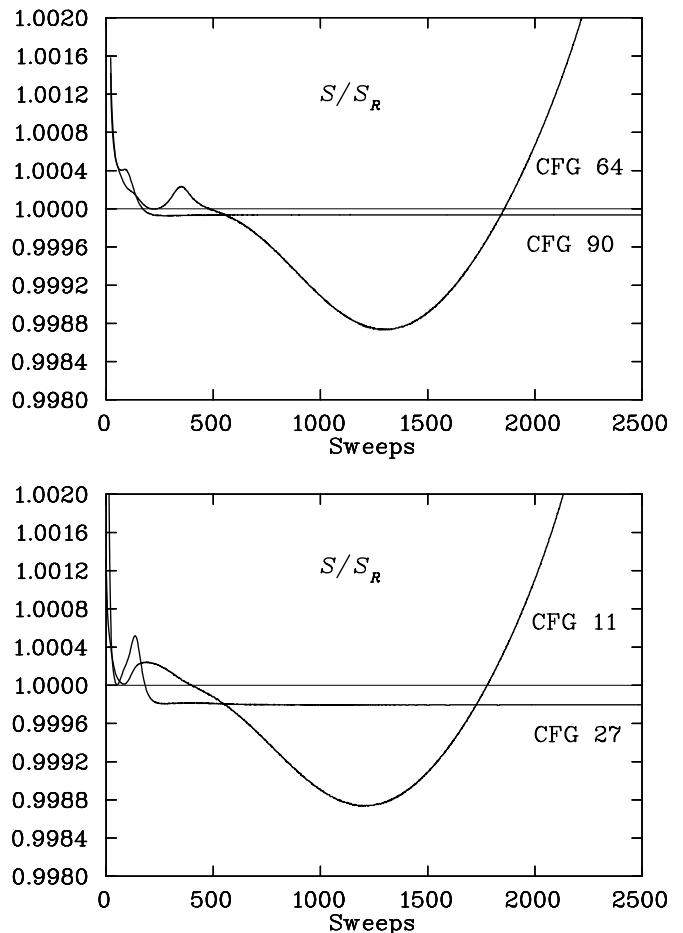

FIG. 8: Ratio of the cooling action to the reconstructed action for configurations 64 and 90 (top) and 11 and 27 (bottom). Configurations 11 and 64 are $|Q| \simeq 1$ configurations, whereas configurations 27 and 90 are $|Q| = 2$ configurations.

present.

Early in the cooling evolution, peaks in S/S_R are seen to be associated with the disappearance with topological structures as illustrated in Fig. 6. In the case of the single-instanton configurations, the ratio of the cooling action to reconstructed action, S/S_R, diverges from unity slowly during the middle stages of the cooling process. The point where this ratio starts falling below 1 corresponds to the beginning of the cresting behavior of $|Q|$ which was identified for the $|Q| = 1$ configurations in Section IV A . This corresponds to the early stage where the difference between the size evolutions of the $|Q| = 1$ and $|Q| = 2$ configurations becomes clear. Also, the position of the valley in the ratio S/S_R corresponds to the peak of the cresting of the topological charge illustrated in Figs. 2 and 3.

Finally, S/S_R diverges rapidly as the object present in each configuration falls through the lattice. As the instanton shrinks, the $\mathcal{O}(a^6)$ errors overwhelm the improved action operator and large errors allow the disap-

pearance of the object. By contrast, in the two $|Q| = 2$ configurations the ratio S/S_R remains within 0.02% of unity indefinitely.

V. CONCLUSIONS

In this paper we have compared the cooling of $|Q| = 1$ and $|Q| = 2$ configurations in $SU(3)$ gauge theory, using improved lattice actions and precise monitoring of the sizes of the topological objects and of the lattice discretization errors. In the continuum it is not possible to have a self-dual $|Q| = 1$ configuration on the untwisted four-torus [11], and the results from our lattice analysis suggests three distinct signals, each of which occurs very early in the cooling process, that the $|Q| = 1$ configurations behave differently from the $|Q| = 2$ ones, and that they will ultimately shrink to below the discretization threshold and then disappear much later in the cooling process. These instability signals occur at a stage in the cooling when the topological objects are still much larger than the lattice discretization threshold. None of these signals is present for the $|Q| = 2$ configurations we studied, even though these consisted of two isolated single instantons. This fact is a clear indication that these $|Q| = 1$ instability signals are reflecting the *global* properties of the torus, which is the essence of the continuum torus result [11], rather than *local* effects such as those that ultimately cause a very small $|Q| = 1$ object to fall through the lattice due to discretization errors.

The three instability signals we have found to be characteristic of the $|Q| = 1$ configurations are as follows. First, there is a cresting behavior of the topological charge $|Q|$ away from its precise integer value of 1, as shown in Figures 2 and 3. This does not happen for the $|Q| = 2$ configurations, as shown in Figures 4 and 5. Second, for the $|Q| = 1$ configurations there is an initial swelling of the size of the would-be instanton, but then a steady shrinkage begins at the same point where the cresting in $|Q|$ is observed. This is illustrated in Figure 6. Once again, this is completely different from the behavior for the $|Q| = 2$ configurations, which is shown in Figure 7. The third signal is that for the $|Q| = 1$ configurations the ratio S/S_R of the cooling action to the reconstructed action begins a steady fall below one, before bottoming out and eventually diverging much later in the cooling process, as shown in Figure 8. This deviation below a ratio of 1 begins at the same point, early in the cooling process, where the cresting of $|Q|$ and the rapid shrinkage of the object begin. This is also very different from the behavior of the $|Q| = 2$ configurations, already at this early stage where the topological objects are large.

These results suggest the following picture of the instability, and ultimate disappearance, of $|Q| = 1$ configurations under cooling. The first stage sees the rapid growth and disappearance of temporary peak structures. The second stage, whose onset is indicated by the three sig-
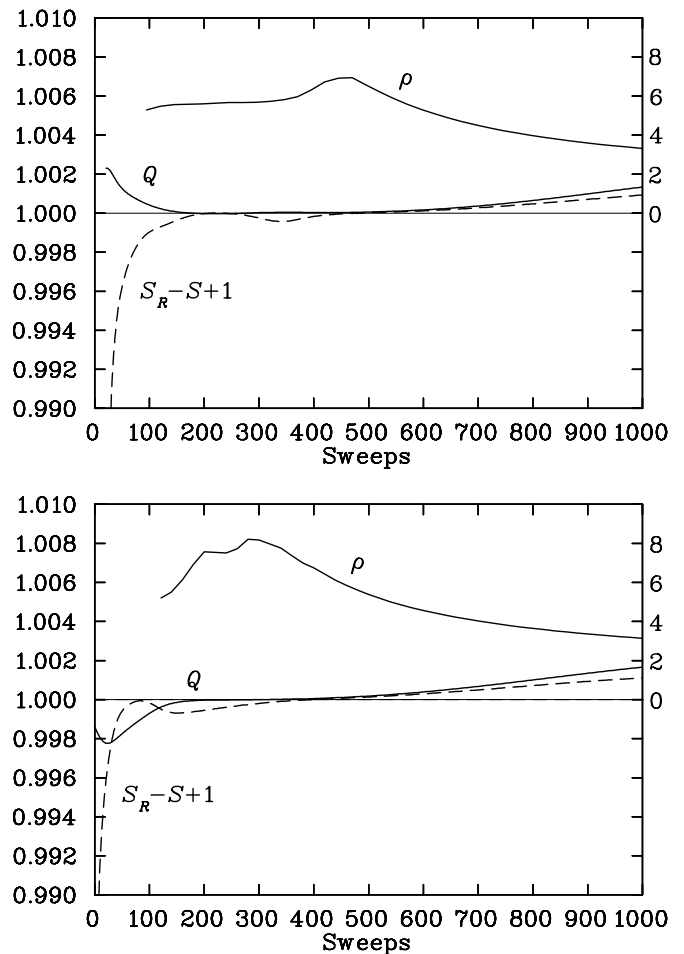

FIG. 9: The behavior of instanton peak size, ρ (upper solid line, right scale), against topological charge (lower solid line, left scale) and $S_R - S + 1$ (dashed line, left scale), as a function of sweep number, for $|Q| \simeq 1$ configurations 64 (upper figure) and 11 (lower figure). Notice that $S_R - S + 1$ and Q move away from integer values at the same time that the instanton starts to shrink. Cooling is performed with the $S(3)$ action, and the topological charge is $Q(3)$. We have taken the value $S_R - S + 1$ rather than $S_R - S$ so that the action and charge curves can be plotted on the same precise scale.

nals listed in the previous paragraph, sees the shrinkage with cooling of the single instanton. This type of shrinkage does not happen for the separate constituents of the $|Q| = 2$ configurations. During this shrinkage stage the topological charge deviates slightly from its integer value of 1. The third and final stage is the rapid disappearance of the single instantons due to dislocation errors at an instanton size of approximately two lattice spacings.

To emphasize these points, we show in Fig. 9 the instanton size ρ, the topological charge Q, and the difference $S_R - S + 1$ between the reconstructed action and cooling action for the $|Q| = 1$ configurations 64 and 11 in the region where the Nahm transform corollary manifests itself. (The addition of one unit to the difference serves

to plot the action and charge curves on the same precise scale.) Since S_R and S have different $\mathcal{O}(a^6)$ errors, their difference is an extremely effective probe of the scale of discretization errors in the configuration. As the instanton changes from expanding behavior to shrinking behavior, the topological charge and difference $S_R - S + 1$ are both almost identically equal to one, indicating minimal discretization errors at the onset of the Nahm transform corollary. This strongly suggests that the sudden change in behavior of the would-be instanton is due to the global nature of the field on the toroidal lattice, and not to local discretization errors.

The $|Q| = 2$ configurations behave very differently from the $|Q| = 1$ configurations. For each of the two $|Q| = 2$ configurations we studied, the configuration consisted of two isolated lumps that drift apart under cooling and have the remarkable property that one lump shrinks, while the other swells, until they reach the same size. It would be interesting to know if this behavior is generic, due to some torus periodicity-induced balance, and if there is any trace of such behavior in the continuum. Unfortunately, this final question is a difficult one, as there are no known nontrivial (*i.e.* inhomogeneous) analytic torus instantons.

We close by noting that all five criteria outlined in the introduction have been met. In particular:

1. The S(3) cooling action is very accurate with remaining errors positive, acting to stabilize topological structure.

2. The action and topological charge density of the $|Q| \simeq 1$ configurations are seen to be distributed over large length scales of 7 to 8 lattice spacings, much larger than the dislocation threshold of the improved cooling algorithm at 2.2 lattice spacings.

3. Comparisons of the reconstructed action with the more traditionally constructed improved action have provided a powerful way of investigating the scale of discretization errors in the configurations under investigation.

4. $|Q| = 1$ configurations have been shown to be stable until the action S drops below $3\,S_0$ and approaches the self-dual limit of $S_0 = 8\pi^2/g^2$. Extra peaks in the action density disappear as S/S_0 drops from 3 toward 1.

5. Finally, the action and topological charge distributions are seen to approach the classical instanton form with only a single peak appearing and the instanton scale parameter $\xi \to 1$ as cooling proceeds.

[1] R. Jackiw, "Quantum Meaning Of Classical Field Theory," Rev. Mod. Phys. **49**, 681 (1977).

[2] G. 't Hooft, "How Instantons Solve The U(1) Problem," Phys. Rept. **142**, 357 (1986).

[3] M. A. Shifman, *Instantons In Gauge Theories*, (World Scientific, Singapore, 1994).

[4] T. Schafer and E. V. Shuryak, "Instantons in QCD," Rev. Mod. Phys. **70**, 323 (1998) [arXiv:hep-ph/9610451].

[5] P. van Baal, "The QCD vacuum," Nucl. Phys. Proc. Suppl. **63**, 126 (1998) [arXiv:hep-lat/9709066].

[6] For an excellent review, see: A. Gonzalez-Arroyo, "Yang-Mills fields on the 4-dimensional torus. (Classical theory)," in *Advanced school on non-perturbative quantum field physics*, M. Asorey and A. Dobado (Eds.), (World Scientific, Singapore, 1998) 57-91; arXiv:hep-th/9807108.

[7] A. A. Belavin, A. M. Polyakov, A. S. Shvarts and Y. S. Tyupkin, "Pseudoparticle Solutions Of The Yang-Mills Equations," Phys. Lett. B **59**, 85 (1975).

[8] M. F. Atiyah, N. J. Hitchin, V. G. Drinfeld and Y. I. Manin, "Construction Of Instantons," Phys. Lett. A **65**, 185 (1978).

[9] G. 't Hooft, "Some Twisted Selfdual Solutions For The Yang-Mills Equations On A Hypertorus," Commun. Math. Phys. **81**, 267 (1981); P. van Baal, "SU(N) Yang-Mills Solutions With Constant Field Strength On T*4," Commun. Math. Phys. **94**, 397 (1984).

[10] C. Taubes, "Self-dual connections on 4-manifolds with indefinite intersection matrix", *J. Diff. Geom.* **19**, 517-560 (1984).

[11] P. J. Braam and P. van Baal, "Nahm's Transformation For Instantons," Commun. Math. Phys. **122**, 267 (1989).

[12] W. Nahm, "A Simple Formalism For The Bps Monopole," Phys. Lett. B **90**, 413 (1980); "Selfdual Monopoles And Calorons," *Presented at 12th Colloq. on Group Theoretical Methods in Physics, Trieste, Italy, Sep, 1983*, G. Denardo et al (Eds.), Lecture Notes in Physics, 201, (Springer-Verlag, Berlin, 1984)

[13] P. van Baal, "Instanton moduli for T(3) x R," Nucl. Phys. Proc. Suppl. **49**, 238 (1996) [arXiv:hep-th/9512223].

[14] A. Gonzalez-Arroyo, "On Nahm's transformation with twisted boundary conditions," Nucl. Phys. B **548**, 626 (1999) [arXiv:hep-th/9811041].

[15] G. 't Hooft, "A Property Of Electric And Magnetic Flux In Nonabelian Gauge Theories," Nucl. Phys. B **153**, 141 (1979). Hypertorus," Commun. Math. Phys. **85**, 529 (1982); P. van Baal, "Twisted Boundary Conditions: A Nonperturbative Probe For Pure Nonabelian Gauge Theories," PhD Thesis, Utrecht U., 1984, INIS-mf-9631.

[16] A. Gonzalez-Arroyo and C. Pena, "Nahm transformation on the lattice," JHEP **9809**, 013 (1998) [arXiv:hep-th/9807172], "Nahm transformation on the lattice," Nucl. Phys. Proc. Suppl. **83**, 533 (2000) [arXiv:hep-lat/9909016].

[17] M. Garcia Perez, A. Gonzalez-Arroyo, C. Pena and P. van Baal, "Nahm dualities on the torus: A synthesis," Nucl. Phys. B **564**, 159 (2000) [arXiv:hep-th/9905138].

[18] M. Garcia Perez, A. Gonzalez-Arroyo and C. Pena, "Perturbative construction of self-dual configurations on the torus," JHEP **0009**, 033 (2000) [arXiv:hep-th/0007113].

[19] P. de Forcrand, M. Garcia Perez and I. O. Stamatescu, "Topology of the SU(2) vacuum: A lattice study using improved cooling," Nucl. Phys. B **499**, 409 (1997) [arXiv:hep-lat/9701012].

[20] P. de Forcrand, M. Garcia Perez and I. O. Stamatescu, "Improved cooling algorithm for gauge theories," Nucl. Phys. Proc. Suppl. **47**, 777 (1996) [arXiv:hep-lat/9509064]; "Topology by improved cooling: Susceptibility and size distributions," Nucl. Phys. Proc. Suppl. **53**, 557 (1997) [arXiv:hep-lat/9608032].

[21] K. Symanzik, "Continuum Limit And Improved Action In Lattice Theories. 1. Principles And Phi*4 Theory," Nucl. Phys. B **226**, 187 (1983).

[22] S. O. Bilson-Thompson, D. B. Leinweber and A. G. Williams, "Highly-improved lattice field-strength tensor," Annals Phys. **304**, 1 (2003) [arXiv:hep-lat/0203008].

[23] M. Garcia Perez, A. Gonzalez-Arroyo, J. Snippe and P. van Baal, "Instantons From Over - Improved Cooling," Nucl. Phys. B **413**, 535 (1994) [arXiv:hep-lat/9309009].

[24] K. G. Wilson, "Confinement Of Quarks," Phys. Rev. D **10**, 2445 (1974).

[25] G. P. Lepage, "Redesigning lattice QCD," In *Schladming 1996, Perturbative and nonperturbative aspects of quantum field theory*, H. Latal and W. Schweiger (Eds.), Lecture Notes in Physics **479**, 1-48, (Springer-Verlag, Berlin, 1997); arXiv:hep-lat/9607076.

[26] Here we correct a typographical error in Ref. [22] where the normalization was incorrectly stated as 1/2 as opposed to 1/12.

[27] N. Cabibbo and E. Marinari, "A New Method For Updating SU(N) Matrices In Computer Simulations Of Gauge Theories," Phys. Lett. B **119**, 387 (1982).

[28] F. D. Bonnet, D. B. Leinweber, A. G. Williams and J. M. Zanotti, "Improved smoothing algorithms for lattice gauge theory," Phys. Rev. D **65**, 114510 (2002) [arXiv:hep-lat/0106023].

[29] F. D. Bonnet, D. B. Leinweber and A. G. Williams, "General algorithm for improved lattice actions on parallel computing architectures," J. Comput. Phys. **170**, 1 (2001) [arXiv:hep-lat/0001017].

[30] D. J. Kusterer, J. Hedditch, W. Kamleh, D. B. Leinweber and A. G. Williams, "Low-lying eigenmodes of the Wilson-Dirac operator and correlations with topological objects," Nucl. Phys. B **628**, 253 (2002) [arXiv:hep-lat/0111029].

[31] M. Garcia Perez, T. G. Kovacs and P. van Baal, "Comments on the instanton size distribution," Phys. Lett. B **472**, 295 (2000) [arXiv:hep-ph/9911485]; "Overlapping instantons," arXiv:hep-ph/0006155, Published in Proceedings of *Continuous advances in QCD, 2000*, pp 79-89, M.B. Voloshin (Ed.), (World Scientific, Singapore, 2001).